



# Qualitative real-time range extraction for preplanned scene partitioning using laser beam coding

Didi Sazbon <sup>a,\*</sup>, Zeev Zalevsky <sup>b</sup>, Ehud Rivlin <sup>a</sup>

<sup>a</sup> Department of Computer Science, Technion—Israel Institute of Technology, Technion City, Haifa 32000, Israel

<sup>b</sup> School of Engineering, Bar-Ilan University, Israel

Received 21 September 2004; received in revised form 20 February 2005

Available online 29 April 2005

Communicated by R. Davies

---

## Abstract

This paper proposes a novel technique to extract range using a phase-only filter for a laser beam. The workspace is partitioned according to  $M$  meaningful preplanned range segments, each representing a relevant range segment in the scene. The phase-only filter codes the laser beam into  $M$  different diffraction patterns, corresponding to the predetermined range of each segment. Once the scene is illuminated by the coded beam, each plane in it would irradiate in a pattern corresponding to its range from the light source. Thus, range can be extracted at acquisition time. This technique has proven to be very efficient for qualitative real-time range extraction, and is mostly appropriate to handle mobile robot applications where a scene could be partitioned into a set of meaningful ranges, such as obstacle detection and docking. The hardware consists of a laser beam, a lens, a filter, and a camera, implying a simple and cost-effective technique.

© 2005 Elsevier B.V. All rights reserved.

*Keywords:* Range estimation; Laser beam coding

---

## 1. Introduction

Range estimation is a basic requisite in Computer Vision, and thus, has been explored to a

great extent. One can undoubtedly find a large quantity of range estimation techniques. These techniques vary in characteristics, such as: density, accuracy, cost, speed, size, and weight. Each technique could be suitable to a group of application, and at the same time, completely inappropriate to others. Therefore, the decision of matching the best technique usually depends on the specific requirements of the desired application. For

---

\* Corresponding author. Tel.: +972 4 8266077; fax: +972 4 8293900.

E-mail address: [didi@cs.technion.ac.il](mailto:didi@cs.technion.ac.il) (D. Sazbon).

example: 3D modeling of an object might need both dense and accurate estimation, where cost and speed would not be critical. On the contrary, dense and accurate estimation might have less importance in collision-free path planning, where cost, speed, and mobility, would be essential.

Range sensing techniques can be divided into two categories: passive and active (Jarvis, 1983, 1993). Passive sensing refers to techniques using the environmental light conditions, such that do not impose artificial energy sources. These techniques include: range from focus/defocus, range from attenuating medium, range from texture, range from stereo, and range from motion. Active sensing refers to techniques that impose structured energy sources, such as: light, ultrasound, X-ray, and microwave. These techniques include: ultrasonic range sensors, radar range sensors, laser sensors (time-of-flight), range from brightness, pattern light range sensors (triangulation), grid coding, and Moiré fringe range contours.

The technique presented here fits in the pattern light category. Pattern light is commonly used in a stereo configuration in order to facilitate the correspondence procedure, which forms the challenging part of triangulation. Usually, one camera is replaced by a device that projects pattern light (also known as ‘structure light’), while the scene is grabbed by the other camera. A very popular group of techniques are known as ‘coded structured light’. The coding is achieved either by projecting a single pattern or a set of patterns. The main idea is that the patterns are designed in such a way that each pixel is assigned with a codeword (Salvi et al., 2004). There is a direct mapping between the codeword of a specific pixel and its corresponding coordinates, so correspondence becomes trivial. Different types of patterns are used for the coding process, such as: black and white, gray scale, and RGB (Caspi et al., 1998; Horn and Kiryati, 1999; Manabe et al., 2002; Pages et al., 2003; Sato and Inokuchi, 1987; Valkenburg and McIvor, 1998). Coded structure light is considered one of the most reliable techniques for estimating range, but since usually a set of patterns is needed, it is not applicable to dynamic scenes. When using only one pattern, dynamic scenes

might be allowed, but the results are usually of poor resolution.

Additional techniques implementing structured light to assist the correspondence procedure include sinusoidal varying intensities, stripes of different types (e.g. colored, cut), and projected grids (Albampton and Goshtasby, 2003; Fofi et al., 2003; Furukawa and Kawasaki, 2003; Guisser et al., 2000; Je et al., 2004; Kang et al., 1995; Maruyama and Abe, 1993; Scharstein and Szeliski, 2003). These methods, although projecting only one pattern, still exploit a time consuming search procedure.

Recently, efforts to estimate range using pattern light and only one image were made. In (Winkelbach and Wahl, 2002), objects were illuminated with a stripes pattern, and surface orientation was first estimated from the directions and the width of the stripes. Then shape was reconstructed from orientations. The drawback of this technique is that it works only for a single object, and the reconstruction is relative, i.e. no absolute range is known. In (Lee et al., 1999), Objects were illuminated with a sinusoidal pattern, and depth was calculated from the frequency variation. The drawback of this technique is its heavy computational time.

Here, pattern light is used with only one image to directly estimate range. No correspondence (triangulation) is needed, and the setup consists only of a laser beam, a lens, a single mask, and a camera. The main concept would be to partition the workspace into a set of range segments, in a way that would be meaningful for a working mobile robot. The motivation lies in the fact that in order to perform tasks such as obstacle detection or docking, it should be sufficient that the robot would be able to distinguish between a set of predefined ranges. The idea is to code a laser beam into different patterns, where each pattern corresponds to a specific range segment. Once a scene is illuminated by the coded beam, each patch in it would irradiate with the pattern that corresponds to its range from the light source. The beam coding is merely realized by one special phase-only filter, and consequently, the technique is accurate, fast (hardware solution), cost-effective, and in addition, fits to dynamic scenes.

## 2. Qualitative real-time range extraction for preplanned scene partitioning using laser beam coding

The proposed technique is based on an iterative design of a phase-only filter for a laser beam. The relevant range is divided into  $M$  meaningful planes. Each plane, once illuminated by a laser beam that propagates through the phase-only filter, would irradiate in a different, predetermined, pattern. The pattern that was chosen here consists of gratings in  $M$  different angles (slits), as depicted in Fig. 1. Each range would be assigned with slits having a unique angle. Once a plane is illuminated, it would irradiate with the angular slits pattern that is proportional to its range.

The iterative procedure is based on the Gerchberg–Saxton (GS) algorithm (Gerchberg and Saxton, 1972; Zalevsky et al., 1996), as schematically illustrated in Fig. 2. What follows is a description of the general concept of the algorithm. Assume we have a function denoted by  $f(x, y)$ , then,  $f(x, y)$  could be represented as:

$$f(x, y) = |f(x, y)| \cdot \exp\{i \cdot \phi(x, y)\} \quad (2.1)$$

where,  $|f(x, y)|$  is the amplitude of  $f(x, y)$ , and  $\phi(x, y)$  is the phase of  $f(x, y)$ . We would denote the Fourier transform of  $f(x, y)$  by  $F(u, v)$ , thus:

$$F(u, v) = |F(u, v)| \cdot \exp\{i \cdot \Phi(u, v)\} \quad (2.2)$$

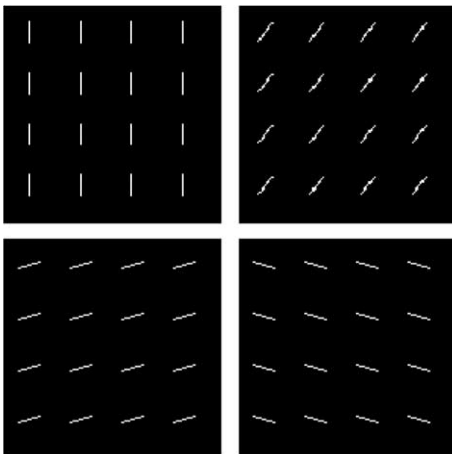


Fig. 1. A pattern of four gratings in different angles, each implying a different range.

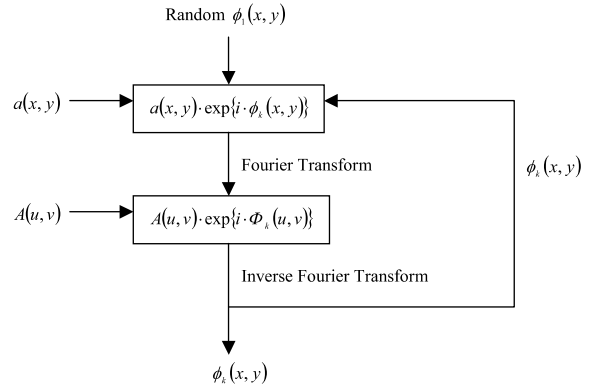


Fig. 2. A schematic description of the GS algorithm to obtain phase information.

where,  $|F(u, v)|$  is the amplitude of  $F(u, v)$ , and  $\Phi(u, v)$  is the phase of  $F(u, v)$ .

Assume  $|f(x, y)|$  and  $|F(u, v)|$  are determined in advance and are denoted by  $a(x, y)$  and  $A(u, v)$ , accordingly. In order to retrieve the phase,  $\phi(x, y)$ , from  $f(x, y)$ , we start with a random estimation of  $\phi(x, y)$ , denoted by  $\phi_1(x, y)$ . Thus,  $f(x, y)$  is estimated by:  $a(x, y) \cdot \exp\{i \cdot \phi_1(x, y)\}$ . The following iterative procedure is performed next, until a satisfactory retrieval is achieved:

1. Fourier transform  $a(x, y) \cdot \exp\{i \cdot \phi_k(x, y)\}$  (the current estimation of  $f(x, y)$ ), resulting in a function denoted by:  $|F_k(u, v)| \cdot \exp\{i \cdot \Phi_k(u, v)\}$ .
2. Replace the magnitude,  $|F_k(u, v)|$ , of the resulted Fourier transform with  $A(u, v)$ , resulting in a function denoted by:  $A(u, v) \cdot \exp\{i \cdot \Phi_k(u, v)\}$ .
3. Inverse Fourier transform  $A(u, v) \cdot \exp\{i \cdot \Phi_k(u, v)\}$ , resulting in a function denoted by:  $a_k(x, y) \cdot \exp\{i \cdot \phi_{k+1}(x, y)\}$ . Note, the phase component is the estimation for the next iteration.
4. Replace the magnitude,  $a_k(x, y)$ , of the resulted Inverse Fourier transform with  $a(x, y)$ , resulting in a new estimation of  $f(x, y)$ , denoted by:  $a(x, y) \cdot \exp\{i \cdot \phi_{k+1}(x, y)\}$ .

Although not proven mathematically, the algorithm is known to give excellent practical results.

If we would like to use the GS concept in order to design a phase-only filter, such that, using a laser beam would result in a predefined pattern,

we would use  $a(x, y) = 1$ , and  $A(u, v)$  will be a function that depicts the desired pattern in which the beam, while propagating in free space, would illuminate. Here, we would like to use that concept, but to create a phase-only filter that would illuminate in a pattern, that slightly changes, as a function of range. Thus, the GS algorithm should be modified to comply with these changes (Levy et al., 1999). The modified procedure is as follows: let  $a(x, y) = 1$ , let  $Z^j(u, v)$  be the pattern assigned to the  $j$ -th plane ( $j = 1, 2, \dots, M$ ), and start with  $\phi_1(x, y)$ , a random estimation of  $\phi(x, y)$ . Proceed with the following iterative procedure:

1. Fourier transform  $a(x, y) \cdot \exp\{i \cdot \phi_k(x, y)\}$ , resulting in a function denoted by:  $A(u, v) \cdot \exp\{i \cdot \Phi_k(u, v)\}$ .
2. Set:  $\tilde{F} = 0$ .
3. Iterate  $M$  times:
  - 3.1. Free space propagate  $A(u, v) \cdot \exp\{i \cdot \Phi_k(u, v)\}$  to the range that is assigned to the pattern denoted by  $Z^j(u, v)$ , and replace the resulted magnitude with  $Z^j(u, v)$ , resulting in a function denoted by  $Z^j(u, v) \cdot \exp\{i \cdot \Phi_k^{\text{FSP}}(u, v)\}$ .
  - 3.2. Free space propagate  $Z^j(u, v) \cdot \exp\{i \cdot \Phi_k^{\text{FSP}}(u, v)\}$  back to the origin, and then, inverse Fourier transform it, resulting in a function denoted by:  $z^j(x, y) \cdot \exp\{i \cdot \phi_k^j(x, y)\}$ .
  - 3.3. Add  $z^j(x, y) \cdot \exp\{i \cdot \phi_k^j(x, y)\}$  to  $\tilde{F}$ .
4. Set:  $F_{\text{estimated}} = \frac{\tilde{F}}{M} = z(x, y) \cdot \phi_{k+1}(x, y)$ .
5. Replace the magnitude,  $z(x, y)$ , of  $F_{\text{estimated}}$ , with  $a(x, y)$ , resulting in a new estimation of  $f(x, y)$ , denoted by:  $a(x, y) \cdot \exp\{i \cdot \phi_{k+1}(x, y)\}$ .

This modified procedure is depicted in Fig. 3.

Note the term *Free Space Propagation* used in step 3 of the procedure. The laser beam is propagated to the position of the plane  $Z^j(u, v)$  by multiplying its spatial spectrum using the term:

$$\text{FS}(x, y, d_j) = \exp \left[ \frac{2\pi i \cdot d_j}{\lambda} \sqrt{1 - \left(\lambda \frac{x}{D}\right)^2 - \left(\lambda \frac{y}{D}\right)^2} \right] \quad (2.3)$$

where,  $d_j$  is the range of the plane from the origin,  $\lambda$  is the wave length, and  $D \times D$  are the dimensions

(in meters) of the detected plane. Note also, that the planes parameters (i.e. the number of planes, the size of a plane, the location of a plane, the distances between planes—that could vary, and the patterns to be displayed on the planes) can be defined to meet specific requirements of the phase-only filter.

The expected behavior of the laser beam once illuminated and according to the physical characteristics of it would be as follows. The beam would be homogeneous until it propagates and encounters the first predefined plane, then it would exhibit the first designed slit pattern. It would keep the same pattern while propagating along the first segment until encountering the second predefined plane, then it would exhibit the second designed slit pattern. It would keep the same pattern while propagating along the second segment and so on. When it would meet the last predefined plane, it would keep propagating indefinitely with its corresponding slit pattern.

Note that the range segments can differ in length and the partitioning should not necessarily be uniform. For example, a docking mobile robot would like to decelerate first at 30 m from the target, then at 5 m, and again at 1 m. The resultant phase-only filter would consist of 3 slits patterns, corresponding to the range segments of 1, 5, and 30 m. Thus, each filter should be designed with range segments that meet the needs of the relevant task, the specific working robot, and the particular workspace.

### 3. Results

The proposed technique was tested with a phase-only filter designed to exhibit the patterns depicted by Fig. 4, on six equally spaced planes positioned between 0.5 and 1 meters from the light source. The range between two consecutive planes equals to 0.1 meters. A laser beam having a wave length of  $0.5 \times 10^{-6}$  m (green light) was used. The physical size of the filter is  $4 \times 4$  mm, and the beam was scattered in order to cover the whole filter. By using the technique described in Section 2, the resulted filter has values in the range  $[-\pi, \pi]$ . In order to save in production costs, the

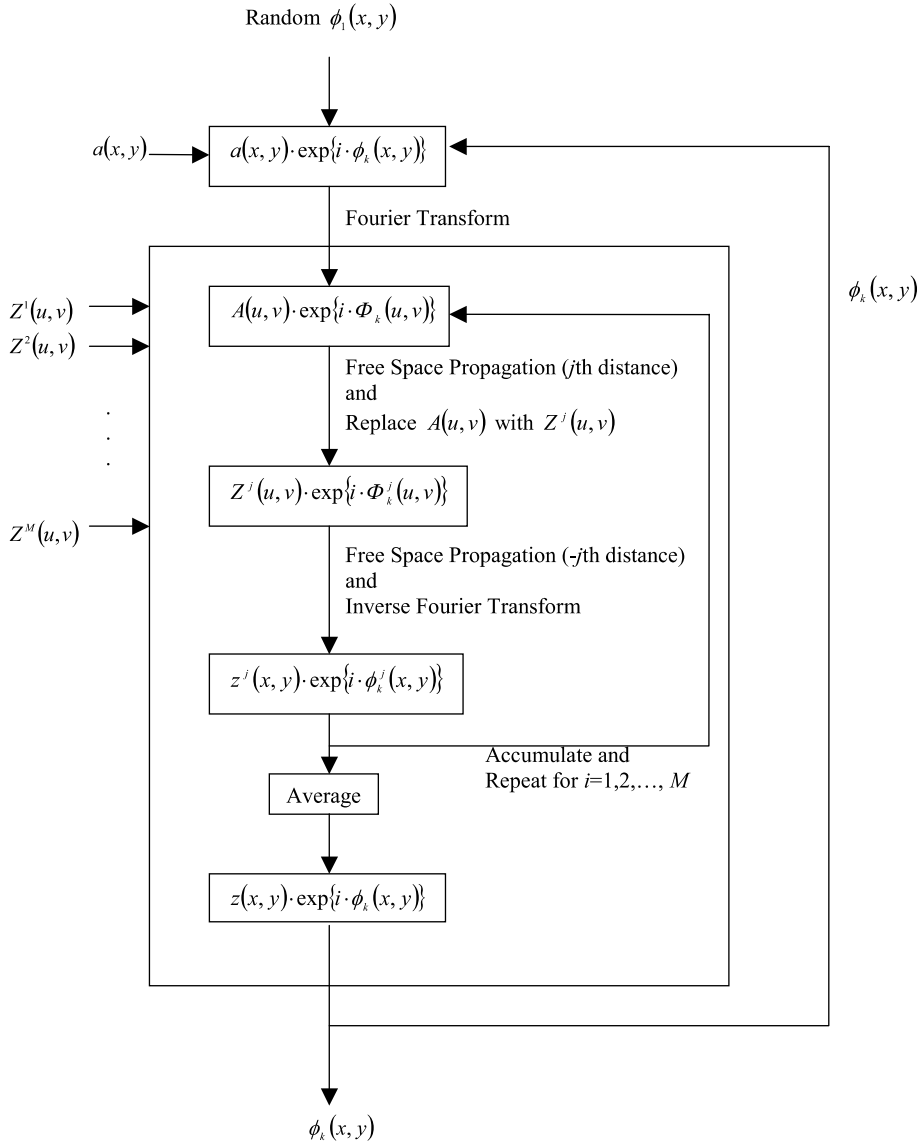


Fig. 3. A schematic description of the modifications to the GS algorithm presented here.

filter was quantized into two levels:  $-\pi$  and 0. As can be seen throughout the experiments, the results are satisfying, while the production is extremely cost effective.

Fig. 5 shows images depicting the patterns irradiated by the phase-only filter on planes positioned at ranges 0.5, 0.6, 0.7, 0.8, 0.9, and 1 m from the light source. Fig. 6 shows enlargements of the

same images around the areas where the irradiation patterns are captured. The directions of the slits are clearly visible to the human eye. In order to automate the application and deduce the range from the assignment of a specific direction to a particular image a simple procedure can be invoked. Fig. 7 demonstrate the simple steps that compose this procedure on Fig. 6b, that was

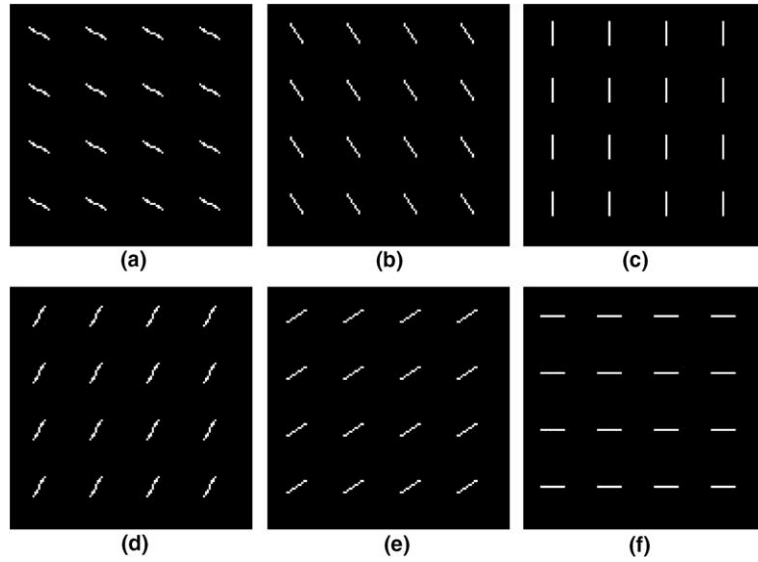


Fig. 4. The patterns that were chosen to irradiate on planes at range: (a) 0.5, (b) 0.6, (c) 0.7, (d) 0.8, (e) 0.9, and (f) 1 m from the light source.

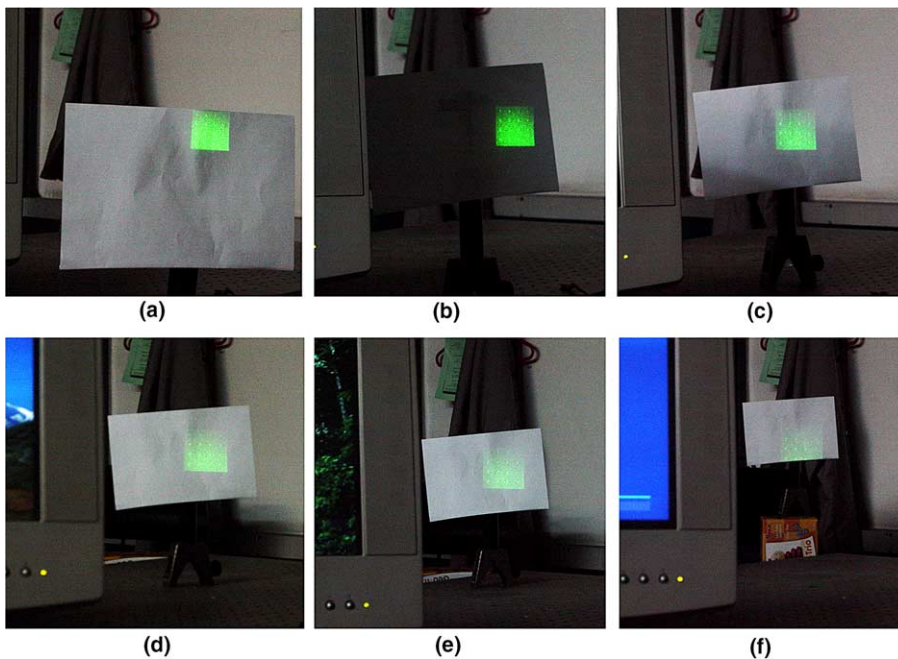


Fig. 5. Images capturing the different patterns irradiating on planes (white paper) at range: (a) 0.5, (b) 0.6, (c) 0.7, (d) 0.8, (e) 0.9, and (f) 1 m from the light source. Note that the plane in image (b) seems to be darker due to the shadow falling from the computer screen placed on the left.

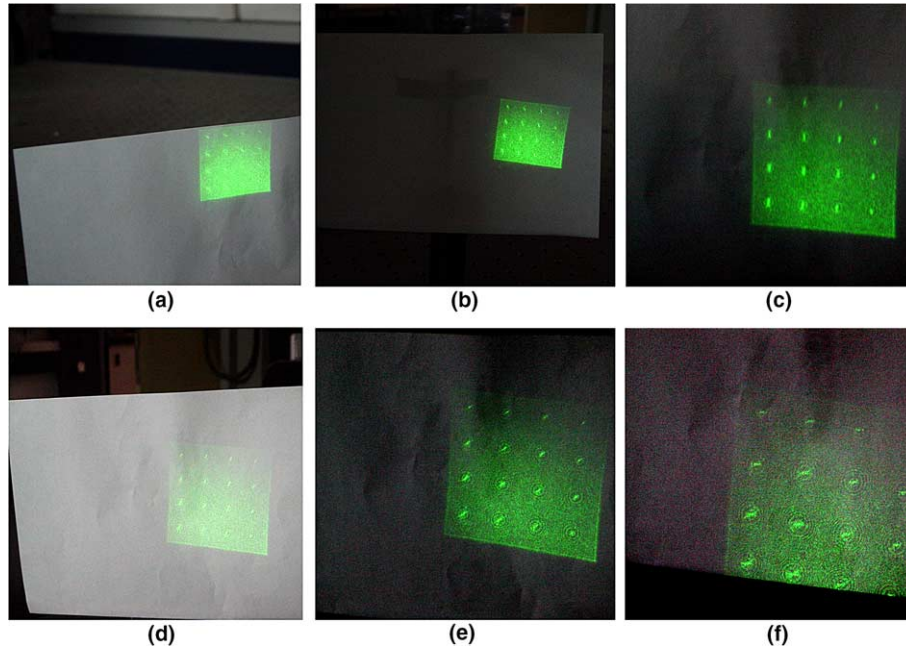


Fig. 6. Enlargements of images (a)–(f) from Fig. 5 around the areas consisting of the irradiation patterns depicting the directions of the slits.

chosen for demonstration. Since these images were taken from a non-calibrated camera they need simple preprocessing.

The first step is depicted in Fig. 7a, and consists of rotating the images, so their patterns would be aligned horizontally, and normalizing their color, so they would be comparable with the correlation patterns. The correlation patterns are merely images of the six possible slits. Then in the next step, taking into considerations the fact that the laser is of bright green color that pops up in the images, a simple threshold is applied, as depicted in Fig. 7b. Note that only the relevant information is now available. The third step is to correlate the image with the six possible patterns (i.e. slits in different directions) to get maximum response on the most compatible one, as depicted in Fig. 7c. Table 1 summarizes the correlation values between the aligned, normalized, and thresholded images depicted in Fig. 6 and the pattern of the slits that corresponds to the images in Fig. 4. As is clearly confirmed, the maximum correlation values correspond to the expected patterns. The numbers in the table are scaled by a constant value.

The accuracy of the specific phase-only filter was also investigated. Recall that the filter was designed to be used in the range between 0.5 and 1 m. As was expected and according to the ‘programming’ of the filter, at distances shorter than 0.5 m no slits pattern were detected. The first pattern appeared at a distance of 0.5 m and kept appearing through the gap between the first and the second predetermined planes. Then, at a distance of 0.6 m, the second pattern appeared and lasted until the following pattern came out, and so on. The last pattern came into sight at a distance of 1 m and stayed on. Following this information, if a match to a certain slit pattern is established, it could be deduced that the irradiating plane is at distance between its corresponding range and lasting through the gap. For example, if the third pattern irradiates, it can be deduced that a plane is present at distance between 0.7 and 0.8 m. Note that the length of the gap can be controlled and determined in advance, so it will meet the needs of the system, at the filter design step.

In addition, we have measured the accuracy of the technique at the border planes where the

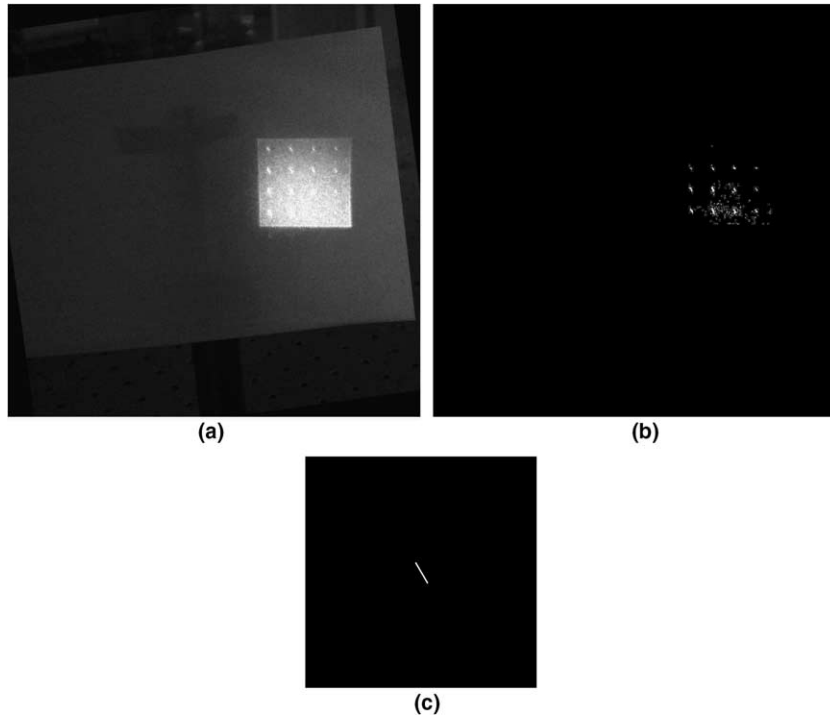


Fig. 7. The steps taken in order to automatically classify the pattern direction demonstrated on image Fig. 6b. (a) The image is aligned horizontally and its color is normalized. (b) A threshold is applied, and since the laser is of bright green color that pops up in its neighborhood, only relevant information remains. (c) The slit pattern that gives maximum correlation response.

Table 1

Correlation values between the aligned, normalized, and thresholded images depicted in Fig. 6 and the pattern of the slits that corresponds to the images in Fig. 4

	Pattern (a)	Pattern (b)	Pattern (c)	Pattern (d)	Pattern (e)	Pattern (f)	Maximum	Should be
Image (a)	2.8815	2.805	1.989	2.2185	2.2695	2.04	Pattern (a)	Pattern (a)
Image (b)	1.0965	1.4535	1.0455	0.918	0.8925	0.714	Pattern (b)	Pattern (b)
Image (c)	1.326	1.887	2.2695	1.7595	1.3005	0.918	Pattern (c)	Pattern (c)
Image (d)	1.4535	1.5555	1.6575	2.0655	1.8105	1.3515	Pattern (d)	Pattern (d)
Image (e)	1.377	1.275	1.326	2.1675	2.3205	1.5045	Pattern (e)	Pattern (e)
Image (f)	1.632	1.275	0.9435	1.377	1.8105	1.836	Pattern (f)	Pattern (f)

As is clearly confirmed, the maximum correlation values correspond to the expected patterns.

patterns were supposed to change, and found out that all the ranges were accurate up to 1–3 mm independently from the range itself. This implies that this specific filter has a reliability of 97% in finding the border ranges. Also, if a robot would be interested in finding out when it is exactly on a border plane, it only needs to find a point of change between two successive patterns. Considering the directions of the two patterns, the range is

directly deduced. Note that, in general, if a different filter would be designed its accuracy and reliability should be measured individually.

Fig. 8 depicts a semi-realistic scene where a mobile robot (the car) illuminates the scene using the proposed phase-only filter in order to detect obstacles. Two boxes, acting as obstacles, are positioned in front of it, and it can be clearly seen that the pattern of the filter is split between both of them,



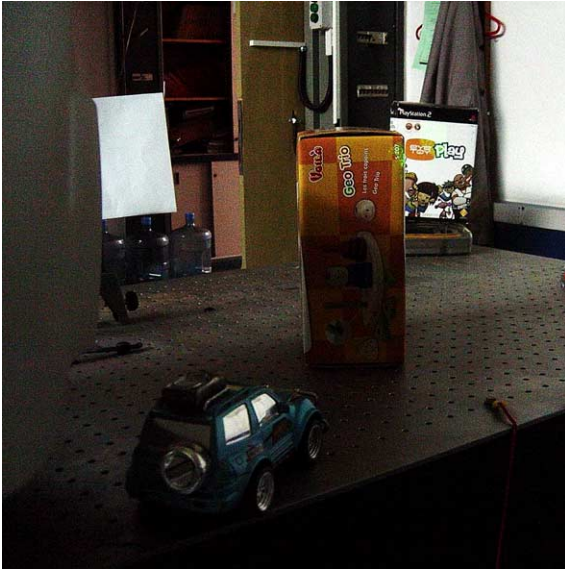


Fig. 8. A semi-realistic scene where a mobile robot (a car) illuminates the scene using the proposed phase-only filter in order to detect obstacles. Two boxes are positioned in front of it, and it can be clearly seen that the pattern of the filter is split between both of them, where one half irradiates in a specific pattern and the other half irradiates in a different pattern.

where one half irradiates in a specific pattern and the other half irradiates in a different pattern. For a better observation, Fig. 9a consists of a closer image of the obstacles, while Fig. 9b and c consist of even closer images of each of the obstacles. By analyzing the patterns it can be deduced that the first obstacle is located at distance between 0.7 and 0.8 m and the second at distance between 0.8 and 0.9 m (in respect to the light source).

The results clearly demonstrate that using the proposed technique, range is determined immediately, in real time. In addition to its accuracy, simplicity, and speed, the technique is extremely cost effective, it comprises only of a laser beam, a lens, a filter, and a common camera.

#### 4. Discussion

A technique to qualitative real-time range estimation for preplanned scene partitioning is presented here. The setup consists of a laser beam, a lens, a single phase-only filter, and a camera. The phase-only filter is designed in such a way, that a scene patch illuminated by it, would irradiate in a unique pattern proportional to its range from the light source. The phase-only filter can be designed to meet the specific parameters of its working environment. Relevant parameter include: the location (range) of the first range segment, the number of range segments, the length of each segment (e.g. shorter for nearby environment), the uniformity of the gaps (e.g. equal, changing), the dimensions of the projected pattern (e.g. 10 cm, 1/2 m), and the density of the slits forming the pattern. If the environmental conditions require a stronger contrast, a stronger laser source can be used. Note, since the physics of propagating light should be taken into considerations, the dimensions of the projected pattern are getting bigger as the range increase.

The specific scanner implemented here and described in the results section, is in fact, a very sim-

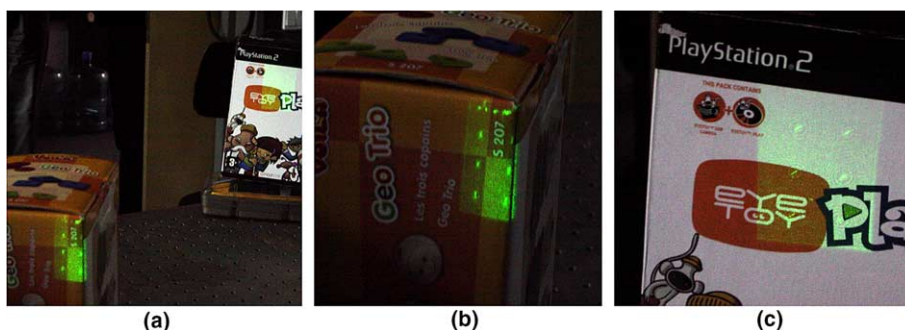


Fig. 9. A closer observation of the scene demonstrated in Fig. 8: (a) depicts both obstacles, while (b) and (c) depict even closer each obstacle.

ple one. It could be assembled using available laboratory components. Thus, its main role in proving the correctness of the technique, and as such it was designed having a relatively short total range (0.5–1 m) with relatively long range segments (0.1 m), best suitable for the task of obstacle detection or docking. The environmental factors that might affect the accuracy or the reliability of this scanner are light conditioning or green obstacles. If the light is too strong, the green slits can be hardly seen. Also, if the scene would consist of green obstacles, it might be difficult to separate the slits from the background. This problem, when appropriate, can be resolved by using a laser beam of red light.

In general, the technique would mostly fit in a context of a mobile robot that would be interested in a rough estimation of a scene structure. This would enable it to identify guidelines in predetermined ranges and consequently, plan its path. The workspace can be partitioned in advance into a set of relevant ranges composed of near, intermediate, and far at the same time, with variable length of segments. Near ranges would naturally be densely segmented, whereas far ranges would be segmented in sparse manner. The robot would have its range partitioned into an appropriate and meaningful warning zones, so when a match is achieved, a corresponding action could be invoked. The technique extremely fits such scenarios by providing both qualitative and reliable results.

## References

- Albamont, J., Goshtasby, A., 2003. A range scanner with a virtual laser. *Image Vision Comput.* 21, 271–284.
- Caspi, D., Kiryati, N., Shamir, J., 1998. Range imaging with adaptive color structured light. *IEEE Trans. PAMI* 20 (5), 470–480.
- Fofi, D., Salvi, J., Mouaddib, E.M., 2003. Uncalibrated reconstruction: An adaptation to structured light vision. *Pattern Recogn.* 36, 1631–1644.
- Furukawa, R., Kawasaki, H., 2003. Interactive shape acquisition using marker attached laser projector, 3DIM'03, 491–498.
- Gerchberg, R.W., Saxton, W.O., 1972. A practical algorithm for the determination of phase from image and diffraction plane pictures. *Optik* 35, 237–246.
- Guisser, L., Payrissat, R., Castan, S., 2000. PGSD: An accurate 3D vision system using a projected grid for surface descriptions. *Image Vision Comput.* 18, 463–491.
- Horn, E., Kiryati, N., 1999. Toward optimal structured light patterns. *Image Vision Comput.* 17 (2), 87–97.
- Jarvis, R.A., 1983. A perspective on range finding techniques for computer vision. *IEEE Trans. PAMI* 5 (2), 123–139.
- Jarvis, R.A., 1993. Range sensing for computer vision. In: Jain, A.K., Flynn, P.J. (Eds.), *Three-dimensional Object Recognition Systems*. Elsevier Science Publishers B.V.
- Je, C., Lee, S.W., Park, R.-H., 2004. High-contrast color-stripe pattern for rapid structured-light range imaging, *ECCV'04*-1, 95–107.
- Kang, S.B., Webb, J.A., Zitnick, C., Kanade, T., 1995. A multibaseline stereo system with active illumination and real-time image acquisition, *ICCV'95*, 88–93.
- Lee, S.-K., Lee, S.-H., Choi, J.-S., 1999. Depth measurement using frequency analysis with an active projection, *ICIP'99*-3, 906–909.
- Levy, U., Shabtay, G., Mendlovic, D., Zalevsky, Z., Marom, E., 1999. Iterative algorithm for determining optimal beam profiles in a 3-D space. *Appl. Opt.* 38, 6732–6736.
- Manabe, Y., Parkkinen, J., Jaaskelainen, T., Chihara, K., 2002. Three dimensional measurement using color structured patterns and imaging spectrograph, *ICPR'02*-3, 649–652.
- Maruyama, M., Abe, S., 1993. Range sensing by projecting multiple slits with random cuts. *IEEE Trans. PAMI* 15 (6), 647–651.
- Pages, J., Salvi, J., Matabosch, C., 2003. Implementation of a robust coded structured light technique for dynamic 3D measurements, *ICIP'03*-3, 1073–1076.
- Salvi, J., Pages, J., Batlle, J., 2004. Pattern codification strategies in structured light systems. *Pattern Recogn.* 37, 827–849.
- Sato, K., Inokuchi, S., 1987. range-imaging system utilizing nematic liquid crystal mask, *ICCV'87*, 657–661.
- Scharstein, D., Szeliski, R., 2003. high-accuracy stereo depth maps using structured light, *CVPR'03*-1, 195–202.
- Valkenburg, R.J., McIvor, A.M., 1998. Accurate 3D measurement using a structured light system. *Image Vision Comput.* 16, 99–110.
- Winkelbach, S., Wahl, F.M., 2002. Shape from single stripe pattern illumination, *DAGM'02*, 240–247.
- Zalevsky, Z., Mendlovic, D., Dorsch, R.G., 1996. The Gerchberg–Saxton algorithm applied in the fractional Fourier or the Fresnel domains. *Opt. Lett.* 21, 842–844.